Published in final edited form as:
Circ Cardiovasc Imaging. 2009 September ; 2(5): 373–381. doi:10.1161/CIRCIMAGING.108.843227.

In Vivo Metabolic Phenotyping of Myocardial Substrate Metabolism in Rodents: Differential Efficacy of Metformin and Rosiglitazone Monotherapy

Kooresh I. Shoghi, PhD[1,*], **Brian N. Finck, PhD**[2], **Kenneth B. Schechtman, PhD**[3], **Terry Sharp**[1], **Pilar Herrero, MS**[1], **Robert J. Gropler, MD**[1], and **Michael J. Welch, PhD**[1]

[1]Mallinckrodt Institute of Radiology, Division of Radiological Sciences, Washington University School of Medicine, St. Louis, Missouri

[2]Department of Medicine, Division of Geriatrics and Nutritional Science, Washington University School of Medicine, St. Louis, Missouri

[3]Division of Biostatistics, Washington University School of Medicine, St. Louis, Missouri

Abstract

Background—Cardiovascular disease is the leading cause of death among diabetic patients with alterations in myocardial substrate metabolism being a likely contributor. We aimed to assess noninvasively the efficacy of Metformin and Rosiglitazone monotherapy in normalizing myocardial substrate metabolism in an animal model of type-2 diabetes mellitus.

Methods and Results—The study utilized 18 male ZDF rats (fa/fa) with 6 rats in each group: an untreated group; a group treated with Metformin (16.6mg/kg/day) and a group treated with Rosiglitazone (4mg/kg). Each rat was scanned at age 14 weeks (baseline) and subsequently at 19 weeks with small animal PET to estimate myocardial glucose utilization (MGU) and myocardial utilization (MFAU), oxidation (MFAO) and esterification (MFAE). Treatment lasted for 5 weeks following baseline imaging. At week 19, rats were sacrificed and hearts extracted for expression analysis of select genes encoding for GLUT transporters and fatty acid transport and oxidation genes. In addition, echocardiography (ECHO) measurements were obtained at week 13 and 18 to characterize cardiac function. Metformin had no significant effect on either MGU or MFAU and MFAO. In contrast, Rosiglitazone tended to enhance MGU and significantly reduced MFAU and MFAO. Rosiglitazone-induced increase in glucose uptake correlated significantly with increased expression of GLUT4 while diminished MFAO correlated significantly with decreased expression of FATP-1 and MCAD. Finally, changes in fractional shortening as a measure of cardiac function were unchanged throughout the study.

Conclusions—Treatment with Rosiglitazone enhanced glucose utilization and diminished MFAO, thus reversing the metabolic phenotype of the diabetic heart.

Keywords

metabolic imaging; type 2 diabetes; gene expression; response to therapy

*__Corresponding author:__ Kooresh Shoghi, Washington University School of Medicine, Mallinckrodt Institute of Radiology, 510 South Kingshighway Blvd., Campus Box 8225, St. Louis, MO 63110, Tel: 314-362-8990, Fax: 314-362-9940, shoghik@wustl.edu.

DISCLOSURES: NONE

INTRODUCTION

Cardiovascular disease is the leading cause of death among diabetic patients [1, 2]. There is increased evidence suggesting that diabetic patients have a predisposition to heart failure resulting from impairment in heart muscle contraction, particularly abnormalities in diastolic function [3]. This condition, termed diabetic cardiomyopathy, is often independent of vascular abnormalities and hypertension and is evident in both type-1 and type-2 diabetic patients. Although several theories have been put forth to explain diabetic cardiomyopathy, evidence has emerged that diabetic cardiomyopathy is at least partly a consequence of severe alterations in myocardial energy metabolism [4, 5]. In particular, insulin resistance in type-2 diabetes mellitus (T2D) shifts the balance of substrate utilization such that the diabetic heart relies almost exclusively on fatty acids for its energy needs [6]. High rates of fatty acid utilization result in accumulation of myocardial lipids and lipid intermediates leading to lipotoxicity of the heart [7, 8].

Anti-diabetes therapies such as Metformin and Rosiglitazone attempt to normalize substrate availability and to restore glycemic control by enhancing insulin sensitivity in the periphery [9]. Metformin, a biguanide, is the most commonly prescribed oral anti-diabetic drug to treat T2D in humans [10]. It is thought to act by decreasing hepatic glucose production through activation of AMP-activated protein kinase (AMPK)[11]. Rosiglitazone, on the other hand, targets the peroxisome proliferator-activated receptor-gamma (PPARγ) nuclear receptor. PPARγ agonists have profound effects on glucose and lipid metabolism. This class of drugs has been shown to improve insulin sensitivity in various animal models [12]. In humans, Rosiglitazone reduces whole-body insulin resistance by its insulin sensitizing effects on liver, skeletal muscle, and adipose tissue [13–15]. Recent studies have shown that Rosiglitazone, but not Metformin, enhance myocardial glucose uptake in diabetic patients by enhancing insulin sensitivity [16, 17]. Little is known, however, about the *in-vivo* efficacy of either Metformin or Rosiglitazone on myocardial fatty acid utilization.

Given the insulin sensitizing properties of Rosiglitazone, we hypothesized that improved insulin-stimulated glucose utilization would result in reduced myocardial fatty acid utilization in the diabetic heart. To that end, we performed multi-parameter small animal PET imaging to assess myocardial glucose and fatty acid utilization in the diabetic heart of ZDF rats longitudinally following treatment with Metformin and Rosiglitazone. Additionally, we monitored changes in cardiac function by echocardiographic measurements. Finally, to validate PET findings and to provide a mechanistic insight, we performed expression analysis of genes encoding proteins involved in glucose and fatty utilization.

MATERIALS & METHODS

All chemicals, unless otherwise stated, were purchased from Aldrich Chemical Co., Inc. Radioactive samples were counted on a Beckman 8000 γ-counter. Small-animal PET was performed on either the microPET® Focus-120 [18] or Focus-220 [19] (Siemens Inc., Knoxville, TN).

Synthesis of Radiopharmaceuticals

FDG is produced routinely in our laboratory with a commercially available module (CTI Molecular Imaging). [^{11}C]Palmitate was synthesized according to published methods [20]. [^{11}C]Acetate is produced routinely in our laboratory with a commercially available acetate module (CTI).

Study Design

The study utilized 18 male ZDF rats (fa/fa) divided randomly into three groups with 6 rats in each group: an untreated group; a group treated with Metformin and a group treated with Rosiglitazone. Untreated ZDF rats were fed Purina Constant Nutrition 5008 while the Metformin and Rosiglitazone groups were provided drugs in the diet at doses of 16.6mg/kg/day and 4mg/kg, respectively, proportional to human doses. Each rat was scanned at 14 weeks of age and subsequently at age of 19 weeks with small animal PET. In addition, echocardiography (ECHO) measurements were obtained at 13 and 18 weeks of age. Treatment was started following the imaging session at week 14. Following the PET imaging session at week 19, rats were sacrificed and hearts extracted for gene expression analysis described below.

Animal Preparation

Animal were prepared for small animal PET imaging as described previously [21]. All animal experiments were conducted in compliance with the Guidelines for the Care and Use of Research Animals established by Washington University's Animal Studies Committee.

Echocardiography (ECHO) Measurements

Non-invasive ultrasound examination of the heart was performed using a Vevo770 Ultrasound System (VisualSonics Inc, Toronto, Ontario, Canada) at ages 13 and 18 weeks as described previously[21]. Measures of left ventricular structure were used for partial volume corrections performed in conjunction with kinetic modeling (see below).

Small Animal PET Imaging Protocol

Five (5) seconds following a bolus injection of the radiopharmaceutical via tail vein, dynamic PET acquisition was started. Each rat was imaged at two time points: once at the age of 14 weeks and again at the age of 19 weeks. The imaging protocol consisted of a 60-minute dynamic acquisition PET with ^{18}FDG (0.5–0.8mCi) to characterize glucose utilization as described earlier [21]; a 20-minute dynamic PET acquisition with [^{11}C]Acetate (0.6–0.8mCi) to quantify MBF and MVO_2; followed by a 20-minute acquisition with [^{11}C]Palmitate (0.6–0.8mCi) to quantify myocardial fatty acid metabolism. During each imaging session, 5–6 whole-blood arterial samples were collected from the femoral artery to measure whole blood glucose (5 μL), free fatty acid (FFA; 20 μL), and insulin (5 μL) levels as well as to correct for the presence of ^{11}C-metabolites, as described below and in detail by Sharp et al. [22]. Finally, heart rates were recorded at baseline and throughout the study. In total, the imaging protocol lasted 3–5 h. Dynamic images were reconstructed using filtered back projection (FBP) with a 2.5 zoom on the heart and 40 frames per imaging session.

Substrate Analysis

All substrate measurements were performed using commercially available, well-documented methods that have been validated in small animals [21, 22]. Substrate and insulin values reported within correspond to values obtained at baseline, just prior to PET imaging.

Metabolite Measurements

During [^{11}C]Acetate and [^{11}C]Palmitate imaging session, arterial whole blood samples were taken at 1, 2, 5, 10, 15, and 20 min post administration of radiopharmaceutical to correct for the contribution of CO_2 to total blood radioactivity counts ($^{11}CO_2$, %) [22, 23].

Data Analysis

Extraction of input function—The input function was reconstructed by applying the hybrid image- and blood- sampling (HIBS) algorithm [24] using whole-blood samples used for $^{11}CO_2$ metabolite correction.

Partial volume correction—Partial-volume corrections were derived as described previously [21] by constructing a digital phantom of the heart for each study based on ECHO measurements.

Estimation of MBF—Myocardial blood flow (MBF) rates were characterized by fitting early [^{11}C]Acetate kinetics (typically up to 1-mintues post-injection) to the flow model as described in an earlier work [25].

Estimation of MVO_2—Myocardial oxygen consumption (MVO_2) was estimated by fitting a mono-exponential (k_{mono}) to the clearance phase of [^{11}C]Acetate kinetics which has been shown to correlate to MVO_2 by the relation $MVO_2=(k_{mono}-0.018901)/0.008892$ [26].

Estimation of Glucose Utilization—Glucose uptake rate and utilization were characterized by performing Patlak graphical analysis [27] on anterolateral myocardial FDG volume of interest (VROI) TAC. After some time $t>t^*$ (typically, last 30-minutes of image acquisition), a linear regression model (of order 1) was optimized against the normalized plasma TAC vs. myocardial tissue VROI. The slope of the linear regression line provides the myocardial glucose uptake rate, MGU_{UpR}, of FDG. Myocardial glucose utilization (MGU) is calculated by $MGU=LC*MGU_{UpR}*[GLU]_P$, where $[GLU]_P$ denotes the peripheral concentration of glucose with a lumped-constant (LC) LC=1 [21].

Estimation of Fatty Acid Utilization—The kinetics of [^{11}C]Palmitate is characterized by the compartmental model depicted in Figure 1 [28, 29]. The model includes 4 compartments characterizing the uptake, beta-oxidation with a rate-constant k_5 (/min), and esterification with a rate-constant k_3 (/min) of palmitate in tissue. Kinetic estimates K_1-k_5 were determined by optimizing 0–15min of PET data against myocardial tissue TAC. Myocardial fatty acid oxidation (*MFAO*, nmol/g/min) is defined as $MFAO=k_5C_2^{(ss)}$ while myocardial fatty acid esterification (MFAE, nmol/g/min) is defined as $MFAE=k_3C_2^{(ss)}$ where $C_2^{(ss)}$ denotes the steady state concentration in the interstitial and cytosolic compartment (C_2) with baseline concentration of FFA ($[FFA]_P$) in plasma substituted for the plasma concentration of [^{11}C] Palmitate. Total myocardial fatty acid utilization (MFAU) is given by MFAU=MFAE+MFAO. Myocardial fatty acid utilization ($MFAU_{UpR}$, mL/g/min), esterification ($MFAE_{UpR}$, mL/g/min), and oxidation uptake rate ($MFAO_{UpR}$, mL/g/min) are defined as the intrinsic capacity (i.e., independent of peripheral effects) of the heart to utilize, esterify (for storage), and oxidize palmitate defined by $MFAU_{UpR}=MFAU/[FFA]_P$, $MFAE_{UpR}=MFAE/[FFA]_P$ and $MFAO_{UpR}=MFAO/[FFA]_P$, respectively.

RNA Isolation and Real-Time RT-PCR

Hearts were frozen at −80°C until RNA was isolated for gene-expression analysis. Total RNA was isolated from heart by using RNAzol B (Tel-test) according the manufacturer's instructions to quantify gene expression of genes encoding for GLUT1, GLUT4, medium-chain acyl-CoA dehydrogenase (MCAD), mitochondrial carnitine palmitoyltransferase-I (mCPT-I), CD36, and fatty acid transport protein (FATP-I). RNA concentration and purity were determined by spectrophotometric absorbency at two dilutions. First-strand cDNA was generated by reverse transcription using 500 ng total RNA and the Applied Biosystems (Foster City, CA) reverse transcription (RT) kit. Real-time RT-PCR was performed using the ABI PRISM 7500 Fast

sequence detection system and TAQMAN Fast Universal master mix (Applied Biosystems, Foster City, CA). Arbitrary units of target gene mRNA were corrected to 36B4 RNA content to control for loading.

Statistical Analysis

Efficacy of Treatment—Treatment effects of Metformin and Rosiglitazine on descriptive data, ECHO measurements, and PET outcome measures were determined by calculating change from baseline (W14) to follow-up (W19) and using one-way Analysis of Variance (ANOVA) for each measure with 3 groups (untreated, Metformin-treated, Rosiglitazone-treated). Statistical contrasts were subsequently used to perform all pairwise comparisons. Differences in gene expression were evaluated by a one-way ANOVA on follow-up measures. Unless otherwise stated, all comparisons are reported as differences in outcome measures from baseline (i.e., W19-W14) between groups, i.e., untreated, Metformin-treated, and Rosiglitazone-treated. A *P* value of $P<0.05$ was considered statistically significant. Statistical calculations were performed using SAS. Data are denoted as mean ± 1 Standard Deviation (SD).

Correlation between ECHO Measurements—The Pearson cross-correlation between ECHO measurements was assessed in the ZDF+Metformin and ZDF-Rosligltazone group as well as for the combined dataset.

Correlation between PET Measures and Gene Expression—PET measures at W19 and corresponding gene expression data were grouped into three groups. In the first and second group, untreated data was combined separately with Metformin and Rosiglitazone treatment data to form two groups, i.e., ZDF/ZDF+MET and ZDF/ZDF+ROSI, primarily to enhance the dynamic range of the data. The third group combined all data at W19, i.e., ZDF/ZDF+MET/ZDF+ROSI. The correlation between PET measures and gene expression data was subsequently evaluated by the Pearson correlation, ρ. A $P<0.05$ was considered significant. Correlations were performed with the statistical package SPSS (SPSS, Inc).

RESULTS

Descriptive data, hemodynamic and blood substrate levels (Table 1)

Untreated ZDF rats are characteristically diabetic at W14 as indicated by elevated levels of HbA1C. Treatment with either Metformin or Rosiglitazone significantly lowered HBA1C levels by approximately 18% ($P=0.0005$) and 39% ($P<0.0001$) relative to untreated rats. Moreover, treatment with Rosiglitazone lowered HbA1C significantly more than Metformin ($P<0.0001$). Despite the reduction in HbA1C following treatment, we did not observe a concomitant reduction in circulating glucose levels following treatment ($P>0.05$). Rosiglitazone-treated ZDF rats gained significantly more weight than untreated ZDF rats ($P<0.0001$) and Metformin-treated rats ($P<0.0001$). There were no statistical differences in heart rate, insulin, FFA, MBF, and MVO_2 measures between age-matched ZDF rats and following treatment.

Echocardiographic (ECHO) Measurements (Table 2)

LVM measures increased significantly ($P<0.05$) in both the Metformin- and Rosiglitazone-groups relative to untreated rats. Additionally, Rosiglitazone significantly enhanced diastolic measures of LVID (LVIDd) in comparison to untreated- and Metformin-treated ZDF rats ($P=0.0127$ and $P=0.025$, respectively) although LVIDd correlated significantly with LVM ($P<0.001$). In general, we did not observe a significant correlation between LVM and weight of ZDF rats, except in the ZDF+ROSI group where the correlation was attributed to clustering of data by weight and LVM (data not shown). When LVM was normalized by weight (LVMI),

changes in LVMI were insignificant following Rosiglitazone treatment. On average, changes LVMI following Metformin treatment were significantly higher than Rosiglitazone treatment (P=0.007) and no treatment (P=0.042), albeit the latter is marginally significant. Finally, percent fractional shortening (FS), a measure of systolic function, was not altered significantly throughout the time-course of the study.

Myocardial Substrate Metabolism

Neither untreated nor Metformin-treated ZDF rats exhibited a significant change in myocardial glucose utilization (MGU) and uptake rate (MGU_{UpR}), although there is a trend for an increase in uptake and utilization with age (Figure 2). The Rosiglitazone-induced increase in MGU_{UpR} was only marginally insignificant in comparison to untreated ZDF rats (P=0.06) (Figure 2) with a net relative increase in MGU_{UpR} of 142% in comparison to untreated rats. Similar to the pattern of glucose metabolism, neither untreated nor Metformin-treated ZDF rats displayed a significant change in $MFAU_{UpR}$ (Figure 3A). Rosiglitazone-treated rats, however, exhibited a significant reduction in $MFAU_{UpR}$ compared to untreated ZDF rats (P=0.016) and Metformin-treated rats (P=0.024). The relative difference in reduction of $MFAU_{UpR}$ in comparison to untreated and Metformin-treated rats was 76% and 89%, respectively. We did not observe a significant change in MFAE between groups (Figure 3B) suggesting that the fraction of fatty acids that are stored is unchanged. However, $MFAO_{UpR}$ was significantly lower in ZDF rats treated with Rosiglitazone compared to untreated ZDF rats (P=0.0189) and Metformin-treated rats (P=0.01). The combined effect of enhanced glucose uptake rate and reduction in myocardial fatty utilization rate resulted in a significant (P<0.001) net gain in fractional glucose utilization as depicted in Figure 4.

Gene Expression Analysis (Figure 5)

ZDF rats treated with Rosiglitazone exhibited a marginally significant (P=0.04) increase in expression of GLUT1 and over a 2-fold increase in the expression of GLUT4 (P=0.0028). In contrast, Metformin did not alter expression of GLUT1 and GLUT4 significantly (P>0.05) (Figure 4A). Treatment with Metformin also did not significantly alter gene expression of fatty acid transporters CD36 and FATP-I (P>0.05). Treatment with Rosiglitazone, however, significantly down-regulated expression of FATP-I relative to untreated and Metformin-treated ZDF rats (P=0.014 and P=0.0375, respectively) while gene expression of CD36 was unchanged. Additionally, Rosiglitazone-treated rats exhibited a significant decrease in expression of MCAD relative to untreated ZDF rats (P=0.03) and Metformin-treated ZDF rats (P=0.0388). We did not observe significant differences (P<0.05) in the expression of the gene encoding for mCPT-I. Finally, the expression of PPARα and its cardiac-enriched coactivator protein PGC-1α were not significantly altered (P>0.05) by either Rosiglitazone or Metformin treatment.

Correlation between PET Measures and Gene Expression (Table 3)

In the combined ZDF/ZDF+Met dataset, MGU_{UpR} significantly correlated with GLUT1 (P=0.027) while $MFAO_{UpR}$ measures significantly correlated with gene expression of CD36 (P=0.018) and mCPT-I (P=0.007). In the combined ZDF/ZDF+Rosi dataset, MGU_{UpR} highly correlated with gene expression of GLUT4 (ρ=0.71, P=0.007). In addition, $MFAO_{UpR}$ significantly correlated with gene expression of FATP1 (ρ=0.74, P=0.004) and MCAD (ρ=0.71, P=0.007) with a high correlation between gene expression of FATP1 and MCAD (ρ=0.87, P=0.001) (not shown). Finally, when all 3 groups (ZDF/ZDF+Met/ZDF+Rosi) were combined, we observed no significant correlation between MGU_{UpR} and GLUT1 gene expression (ρ=0.40, P=0.07). In contrast, MGU_{UpR} remained significantly correlated with gene expression of GLUT4 (ρ=0.55, P=0.017) while $MFAO_{UpR}$ remained significantly correlated

with FATP-I (ρ=0.48, P=0.03), albeit the correlation is slightly lower in comparison to values obtained using the ZDF/ZDF+Rosi dataset.

DISCUSSION

The metabolic phenotype of the diabetic heart is characterized by impairments in myocardial glucose uptake and oxidation and overreliance on fatty acids for energy production [30] as reflected in the complex interplay in insulin resistance in both peripheral tissues and heart. The detrimental effects of this metabolic shift include an increased susceptibility to ischemia, enhanced reactive oxygen species production, and the potential for accumulation of myocardial lipids and lipid intermediates leading to lipotoxicity of the heart [7]. Therapeutic interventions are designed primarily to achieve a level of glycemic control and treatment of other co-morbidities such as hyperlipidemia and hypertension. However, even though several classes of anti-diabetic agents may improve glucose homeostasis and insulin sensitivity their impact on myocardial substrate may differ. In this work, we used small animal PET to assess, non-invasively, the efficacy of human-dose-equivalence of Metformin and Rosiglitazone in reversing alterations in myocardial glucose and fatty acid utilization in the ZDF rat.

Rosiglitazone-induced myocardial glucose uptake in ZDF rat (Figure 2) is consistent with observations in diabetic patients [16, 17] and perfused heart studies [31]. Since MGU_{UpR} is independent of plasma glucose levels it provides a lumped measure for the machinery involved in glucose utilization, such as levels of GLUT. We showed that the decline in MGU_{UpR} was associated with low expression of gene encoding for GLUT4 [21]. Indeed, several studies have shown that decreased glucose uptake is linked to decreased GLUT4 protein and mRNA levels [32] in type 1 diabetes and various models of type 2 diabetes [33, 34]. In agreement with PET data, gene expression analysis suggests that Rosiglitazone-induced PPARγ activation resulted in elevated GLUT4, and to a lesser extent, GLUT1 (Figure 5A), confirming previous reports where Rosiglitazone was shown to increase myocardial gene expression of GLUT1 and GLUT4 in ZDF rats [31]. The significant correlation between MGU_{UpR} and gene expression measures of GLUT further supports their association (Table 3).

Our data indicates that in parallel to increased glucose utilization, Rosiglitazone but not Metformin significantly reduced MFAU (Figure 3). The observation that MFAE is unaltered following treatment suggests that the decrease is MFAU is attributed primarily to inhibition of MFAO in cardiac muscle. Interestingly, in a recent study Rosiglitazone enhanced fatty oxidation in skeletal muscle although glucose utilization in the same study was not determined [35]. Considering the potential lipotoxic effects of accumulated fatty acids [7], it can be argued that stimulating fatty acid oxidation in muscle can decrease fatty acid storage and therefore increase insulin-stimulated glucose uptake. However, myocardial fatty acid and glucose utilization rates are almost always reciprocal. Randle and colleagues originally demonstrated that high level fatty acid utilization is associated with diminished glucose utilization in rat heart and vice versa [36]. Thus, one interpretation of the present study is that Rosiglitazone caused a metabolic shift by blunting the heightened uptake and oxidation of fatty acids resulting in an increase in glucose utilization. However, whether these metabolic effects are primary or secondary due to altered substrate flux or insulin sensitivity remains to be determined.

In order to provide a mechanistic insight into the observed decrease in MFAO in cardiac muscle, we characterized the expression profile of genes involved in FA transport and oxidation as well as PPARα and PGC-1α. Both PPARα and PGC-1α were unaltered with treatment consistent with previous reports[31]. The observations that Rosiglitazone led to a down-regulation of FATP-I, but not FAT/CD36 (Figure 5) is somewhat surprising and may indicate a specific role for each transport system. It is possible that the different transporters direct fatty acids toward distinct intracellular pools. Recent work in transgenic mice suggested that FATP-

I overexpression directed fatty acids primarily toward the oxidation pool [37]. Accordingly, our data indicates that reductions in FATP-I expression correlated with diminished MFAO. On the other hand, both FAT/CD36 and MFAE are unaffected by Rosiglitazone suggesting that fatty acids entering through the FAT/CD36transport system may be directed first towards storage pool or serve as substrates in signal transduction, as has been suggested by others [38]. Thus, additional work using mouse models with specific genetic alterations in the activity of each of these pathways is required to determine the role that fatty acid transport.

In parallel to diminished FATP-I gene expression, Rosiglitazone significantly reduced expression of the gene encoding MCAD, a highly regulated step in mitochondrial β oxidation of fatty acids. Accordingly, cardiac intrinsic measures of myocardial fatty acid oxidation rates, $MFAO_{UpR}$, correlated significantly with both FATP-I and MCAD suggesting that PET measures of $MFAO_{UpR}$ provide a non-invasive measure myocardial fatty acid oxidation. Furthermore, the high correlation between expression of FATP-I and MCAD suggests that the two genes are co-regulated following treatment with Rosiglitazone. Both MCAD and FATP-I are known to be target genes that are activated by PPARs [39]. The observed repression by a PPARγ agonist may, at first glance, seem counterintuitive. However, these results are consistent with previous work [40] and suggest that Rosiglitazone is eliciting its effects on cardiac substrate selection through extra-cardiac effects on whole animal metabolism.

Despite a significant decrease in HbA1C levels, we did not observe a concomitant decrease in peripheral glucose levels which can be attributed to the effects of the anesthetic agent on hepatic glucose production, metabolism, and disposal in the periphery [41]. In addition, we did not observe reductions in plasma FFA with either treatment. Several groups observed reductions in peripheral FFA levels when pre-diabetic ZDF rats (less than 8 weeks old) were treated with either Metformin or PPARγ agonists (such as Troglitazone and Rosiglitazone) [8, 31, 42]; the abovementioned studies were designed to assess the effectiveness of the agents to delay or prevent the onset of diabetes. In contrast, we utilized ZDF rats at age of 14 weeks, which are considered diabetic by all accounts, to assess response to treatment. Indeed, in recent investigations involving diabetic patients undergoing treatment with either Metformin or Rosiglitazone, the authors did not observe reductions in FFA levels while improvements in glucose levels were mixed during either fasting or hyperinsulinaemia states[16, 17, 43, 44]. Thus, the effectiveness of therapeutic agents in lowering peripheral substrate levels may be limited by the severity of the disease and the duration of treatment.

The ECHO data suggests that treatment with either Metformin or Rosiglitazone induced changes in LVM. However, when LVM was normalized by the weight (LVMI), changes in LVMI were insignificant following Rosiglitazone treatment and only marginally significant following Metformin treatment. In addition, since LVIDd correlated with LVM, changes in LVIDd can be attributed to weight gain in the Rosiglitazone treatment group. Fractional shortening (FS), a measure of systolic function, did not improve with either treatment. Furthermore, in an earlier publication we did not observe differences in FS between age-matched ZDF rats and lean littermates [21]. In a recent study, however, Zhou et al [8] assessed myocardial function in ZDF rats following a 13 week treatment with Troglitazone, an anti-diabetic drug of the same class (thiazolidinedione) as Rosiglitazone. The authors noted improvements in FS at 20 weeks compared with untreated rats. In contrast, in this work we report alterations in myocardial substrate metabolism as early as 5 weeks following treatment. Taken together, further studies are needed to characterize the time-delay between metabolic alterations and cardiac function both before onset of disease and following therapy.

In summary, we utilized small animal PET to assess changes in myocardial substrate metabolism following monotherapy with either Metformin or Rosiglitazone. Collectively, our data indicates that the PPARγ agonist Rosiglitazone has profound effects on *in vivo* myocardial

glucose utilization and fatty acid oxidation, which we confirmed against expression profiles of genes involved in glucose transport and fatty acid oxidation. In particular, we demonstrated, non-invasively, that treatment with Rosiglitazone not only increased myocardial glucose utilization but, in addition reduced myocardial fatty acid oxidation, thus reversing the metabolic phenotype of the diabetic heart and resulting in significant fractional net gain in glucose utilization. Finally, our findings underscore both the translational capability and the potential use of PET in assessing the efficacy of therapies on myocardial substrate metabolism *in-vivo*, non-invasively.

Cardiovascular disease is the leading cause of death among diabetic patients. There is increasing evidence suggesting that diabetic patients have a predisposition to heart failure resulting from impairment in heart muscle contraction, particularly abnormalities in diastolic function. One hypothesis argues that the observed abnormalities in diastolic function is a consequence of alterations in myocardial substrate metabolism such that the diabetic heart relies more on fatty acid metabolism than glucose metabolism to meet its energy needs. Increased reliance on fatty acids leads to accumulation of fatty acid intermediates as well as triglycerides resulting in lipotoxicity of the heart. In this work we validated technology to non-invasive assess alterations in myocardial substrate metabolism, allowing to "observe " metabolic alterations *in-vivo* potentially preceding development of abnormalities in diastolic function. Moreover, as treatment strategies aim to restore a level of glycemic control. The methodology allows for non-invasive monitoring of therapeutic efficacy as we have demonstrated in this work.

ACKNOWLEDGMENTS

We thank Nicole Fettig, Lori Strong, Margaret M. Morris, Amanda Roth, Paul Eisenbeis, Ann Stroncek, and Jerrel Rutlin for technical assistance and the Washington University School of Medicine cyclotron staff for synthesis of radiopharmaceuticals. We would also like to thank Dr. Attila Kovacs for echocardiography measurements.

FUNDING SOURCES

This work was supported by NIH/NHLBI grant 2PO1HL13851. Gene expression analyses were also supported by the Adipocyte Biology Core of the Clinical Nutrition Research Unit Core Center (P30 DK56341) at Washington University School of Medicine.

REFERENCES

1. Wilson PW. Diabetes mellitus and coronary heart disease. Endocrinol Metab Clin North Am 2001;30:857–881. [PubMed: 11727403]
2. Stamler J, Vaccaro O, Neaton JD, Wentworth D. Diabetes, other risk factors, and 12-yr cardiovascular mortality for men screened in the Multiple Risk Factor Intervention Trial. Diabetes Care 1993;16:434–444. [PubMed: 8432214]
3. Fang ZY, Prins JB, Marwick TH. Diabetic cardiomyopathy: evidence, mechanisms, and therapeutic implications. Endocr Rev 2004;25:543–567. [PubMed: 15294881]
4. Lopaschuk GD, Belke DD, Gamble J, Itoi T, Schonekess BO. Regulation of fatty acid oxidation in the mammalian heart in health and disease. Biochim Biophys Acta 1994;1213:263–276. [PubMed: 8049240]
5. Lopaschuk GD. Metabolic abnormalities in the diabetic heart. Heart Fail Rev 2002;7:149–159. [PubMed: 11988639]
6. Saddik M, Lopaschuk GD. Triacylglycerol turnover in isolated working hearts of acutely diabetic rats. Can J Physiol Pharmacol 1994;72:1110–1119. [PubMed: 7882174]
7. Borradaile NM, Schaffer JE. Lipotoxicity in the heart. Curr Hypertens Rep 2005;7:412–417. [PubMed: 16386196]

8. Zhou YT, Grayburn P, Karim A, Shimabukuro M, Higa M, Baetens D, Orci L, Unger RH. Lipotoxic heart disease in obese rats: implications for human obesity. Proc Natl Acad Sci U S A 2000;97:1784–1789. [PubMed: 10677535]
9. Inzucchi SE. Oral antihyperglycemic therapy for type 2 diabetes: scientific review. Jama 2002;287:360–372. [PubMed: 11790216]
10. Bailey CJ. Metformin revisited: its actions and indications for use. Diabet Med 1988;5:315–320. [PubMed: 2968877]
11. Towler MC, Hardie DG. AMP-activated protein kinase in metabolic control and insulin signaling. Circ Res 2007;100:328–341. [PubMed: 17307971]
12. Fujita T, Sugiyama Y, Taketomi S, Sohda T, Kawamatsu Y, Iwatsuka H, Suzuoki Z. Reduction of insulin resistance in obese and/or diabetic animals by 5-[4-(1-methylcyclohexylmethoxy)benzyl]-thiazolidine-2,4-dione (ADD-3878, U-63,287, ciglitazone), a new antidiabetic agent. Diabetes 1983;32:804–810. [PubMed: 6354788]
13. Hallsten K, Virtanen KA, Lonnqvist F, Sipila H, Oksanen A, Viljanen T, Ronnemaa T, Viikari J, Knuuti J, Nuutila P. Rosiglitazone but not metformin enhances insulin- and exercise-stimulated skeletal muscle glucose uptake in patients with newly diagnosed type 2 diabetes. Diabetes 2002;51:3479–3485. [PubMed: 12453903]
14. Iozzo P, Hallsten K, Oikonen V, Virtanen KA, Parkkola R, Kemppainen J, Solin O, Lonnqvist F, Ferrannini E, Knuuti J, Nuutila P. Effects of metformin and rosiglitazone monotherapy on insulin-mediated hepatic glucose uptake and their relation to visceral fat in type 2 diabetes. Diabetes Care 2003;26:2069–2074. [PubMed: 12832315]
15. Virtanen KA, Hallsten K, Parkkola R, Janatuinen T, Lonnqvist F, Viljanen T, Ronnemaa T, Knuuti J, Huupponen R, Lonnroth P, Nuutila P. Differential effects of rosiglitazone and metformin on adipose tissue distribution and glucose uptake in type 2 diabetic subjects. Diabetes 2003;52:283–290. [PubMed: 12540598]
16. Hallsten K, Virtanen KA, Lonnqvist F, Janatuinen T, Turiceanu M, Ronnemaa T, Viikari J, Lehtimaki T, Knuuti J, Nuutila P. Enhancement of insulin-stimulated myocardial glucose uptake in patients with Type 2 diabetes treated with rosiglitazone. Diabet Med 2004;21:1280–1287. [PubMed: 15569129]
17. Lautamaki R, Airaksinen KE, Seppanen M, Toikka J, Luotolahti M, Ball E, Borra R, Harkonen R, Iozzo P, Stewart M, Knuuti J, Nuutila P. Rosiglitazone improves myocardial glucose uptake in patients with type 2 diabetes and coronary artery disease: a 16-week randomized, double-blind, placebo-controlled study. Diabetes 2005;54:2787–2794. [PubMed: 16123370]
18. Laforest R, Longford D, Siegel S, Newport DF, Yap J. Performance evaluation of the microPET (R) - FOCUS-F120. Ieee Transactions on Nuclear Science 2007;54:42–49.
19. Tai YC, Ruangma A, Rowland D, Siegel S, Newport DF, Chow PL, Laforest R. Performance evaluation of the microPET focus: a third-generation microPET scanner dedicated to animal imaging. J Nucl Med 2005;46:455–463. [PubMed: 15750159]
20. Welch, MJ.; Wittmer, SL.; Dence, CS.; Tewson, TJ. Radiopharmaceuticals labeled with 11C and 18F: considerations related to the preparation of 11C-palmitate. In: R, JW.; K, KA., editors. Short-Lived Radionuclides in Chemistry and Biology. Vol. Vol 197. Washington, DC: American Chemistry Society Advances in Chemistry Series; 1981. p. 407-417.
21. Shoghi KI, Gropler RJ, Sharp T, Herrero P, Fettig N, Su Y, Mitra MS, Kovacs A, Finck BN, Welch MJ. Time Course of Alterations in Myocardial Glucose Utilization in the Zucker Diabetic Fatty Rat with Correlation to Gene Expression of Glucose Transporters: A Small-Animal PET Investigation. J Nucl Med 2008;49:1320–1327. [PubMed: 18632819]
22. Sharp TL, Dence CS, Engelbach JA, Herrero P, Gropler RJ, Welch MJ. Techniques necessary for multiple tracer quantitative small-animal imaging studies. Nucl Med Biol 2005;32:875–884. [PubMed: 16253813]
23. Dence CS, Herrero P, Schwarz SW, Mach RH, Gropler RJ, Welch MJ. Imaging myocardium enzymatic pathways with carbon-11 radiotracers. Methods Enzymol 2004;385:286–315. [PubMed: 15130745]
24. Shoghi KI, Welch MJ. Hybrid image and blood sampling input function for quantification of small animal dynamic PET data. Nucl Med Biol 2007;34:989–994. [PubMed: 17998103]

25. Herrero P, Kim J, Sharp TL, Engelbach JA, Lewis JS, Gropler RJ, Welch MJ. Assessment of myocardial blood flow using 15O-water and 1–11C-acetate in rats with small-animal PET. J Nucl Med 2006;47:477–485. [PubMed: 16513617]
26. Buxton DB, Nienaber CA, Luxen A, Ratib O, Hansen H, Phelps ME, Schelbert HR. Noninvasive quantitation of regional myocardial oxygen consumption in vivo with [1–11C]acetate and dynamic positron emission tomography. Circulation 1989;79:134–142. [PubMed: 2783396]
27. Patlak CS, Blasberg RG. Graphical evaluation of blood-to-brain transfer constants from multiple-time uptake data. Generalizations. J Cereb Blood Flow Metab 1985;5:584–590. [PubMed: 4055928]
28. Bergmann SR, Weinheimer CJ, Markham J, Herrero P. Quantitation of myocardial fatty acid metabolism using PET. J Nucl Med 1996;37:1723–1730. [PubMed: 8862319]
29. Welch MJ, Lewis JS, Kim J, Sharp TL, Dence CS, Gropler RJ, Herrero P. Assessment of myocardial metabolism in diabetic rats using small-animal PET: a feasibility study. J Nucl Med 2006;47:689–697. [PubMed: 16595504]
30. Taegtmeyer H, McNulty P, Young ME. Adaptation and maladaptation of the heart indiabetes: Part I: general concepts. Circulation 2002;105:1727–1733. [PubMed: 11940554]
31. Golfman LS, Wilson CR, Sharma S, Burgmaier M, Young ME, Guthrie PH, Van Arsdall M, Adrogue JV, Brown KK, Taegtmeyer H. Activation of PPARgamma enhances myocardial glucose oxidation and improves contractile function in isolated working hearts of ZDF rats. Am J Physiol Endocrinol Metab 2005;289:E328–E336. [PubMed: 15797988]
32. Camps M, Castello A, Munoz P, Monfar M, Testar X, Palacin M, Zorzano A. Effect of diabetes and fasting on GLUT-4 (muscle/fat) glucose-transporter expression in insulin-sensitive tissues. Heterogeneous response in heart, red and white muscle. Biochem J 1992;282:765–772. [PubMed: 1554359]
33. Desrois M, Sidell RJ, Gauguier D, King LM, Radda GK, Clarke K. Initial steps of insulin signaling and glucose transport are defective in the type 2 diabetic rat heart. Cardiovasc Res 2004;61:288–296. [PubMed: 14736545]
34. Slieker LJ, Sundell KL, Heath WF, Osborne HE, Bue J, Manetta J, Sportsman JR. Glucose transporter levels in tissues of spontaneously diabetic Zucker fa/fa rat (ZDF/drt) and viable yellow mouse (Avy/a). Diabetes 1992;41:187–193. [PubMed: 1733808]
35. Benton CR, Holloway GP, Campbell SE, Yoshida Y, Tandon NN, Glatz JF, Luiken JJ, Spriet LL, Bonen A. Rosiglitazone increases fatty acid oxidation and fatty acid translocase (FAT/CD36) but not carnitine palmitoyltransferase I in rat muscle mitochondria. J Physiol 2008;586:1755–1766. [PubMed: 18238811]
36. Randle PJ, Garland PB, Hales CN, Newsholme EA. The glucose fatty-acid cycle. Its role in insulin sensitivity and the metabolic disturbances of diabetes mellitus. Lancet 1963;1:785–789. [PubMed: 13990765]
37. Chiu HC, Kovacs A, Blanton RM, Han X, Courtois M, Weinheimer CJ, Yamada KA, Brunet S, Xu H, Nerbonne JM, Welch MJ, Fettig NM, Sharp TL, Sambandam N, Olson KM, Ory DS, Schaffer JE. Transgenic expression of fatty acid transport protein 1 in the heart causes lipotoxic cardiomyopathy. Circ Res 2005;96:225–233. [PubMed: 15618539]
38. Coort SL, Bonen A, van der Vusse GJ, Glatz JF, Luiken JJ. Cardiac substrate uptake and metabolism in obesity and type-2 diabetes: role of sarcolemmal substrate transporters. Mol Cell Biochem 2007;299:5–18. [PubMed: 16988889]
39. Carter ME, Gulick T, Moore DD, Kelly DP. A pleiotropic element in the medium-chain acyl coenzyme A dehydrogenase gene promoter mediates transcriptional regulation by multiple nuclear receptor transcription factors and defines novel receptor-DNA binding motifs. Mol Cell Biol 1994;14:4360–4372. [PubMed: 8007945]
40. Cabrero A, Jove M, Planavila A, Merlos M, Laguna JC, Vazquez-Carrera M. Down-regulation of acyl-CoA oxidase gene expression in heart of troglitazone-treated mice through a mechanism involving chicken ovalbumin upstream promoter transcription factor II. Mol Pharmacol 2003;64:764–772. [PubMed: 12920214]
41. Horber FF, Krayer S, Miles J, Cryer P, Rehder K, Haymond MW. Isoflurane and whole body leucine, glucose, and fatty acid metabolism in dogs. Anesthesiology 1990;73:82–92. [PubMed: 2360744]

42. Sreenan S, Sturis J, Pugh W, Burant CF, Polonsky KS. Prevention of hyperglycemia in the Zucker diabetic fatty rat by treatment with metformin or troglitazone. Am J Physiol 1996;271:E742–E747. [PubMed: 8897863]

43. Karlsson HK, Hallsten K, Bjornholm M, Tsuchida H, Chibalin AV, Virtanen KA, Heinonen OJ, Lonnqvist F, Nuutila P, Zierath JR. Effects of metformin and rosiglitazone treatment on insulin signaling and glucose uptake in patients with newly diagnosed type 2 diabetes: a randomized controlled study. Diabetes 2005;54:1459–1467. [PubMed: 15855334]

44. Tiikkainen M, Hakkinen AM, Korsheninnikova E, Nyman T, Makimattila S, Yki-Jarvinen H. Effects of rosiglitazone and metformin on liver fat content, hepatic insulin resistance, insulin clearance, and gene expression in adipose tissue in patients with type 2 diabetes. Diabetes 2004;53:2169–2176. [PubMed: 15277403]

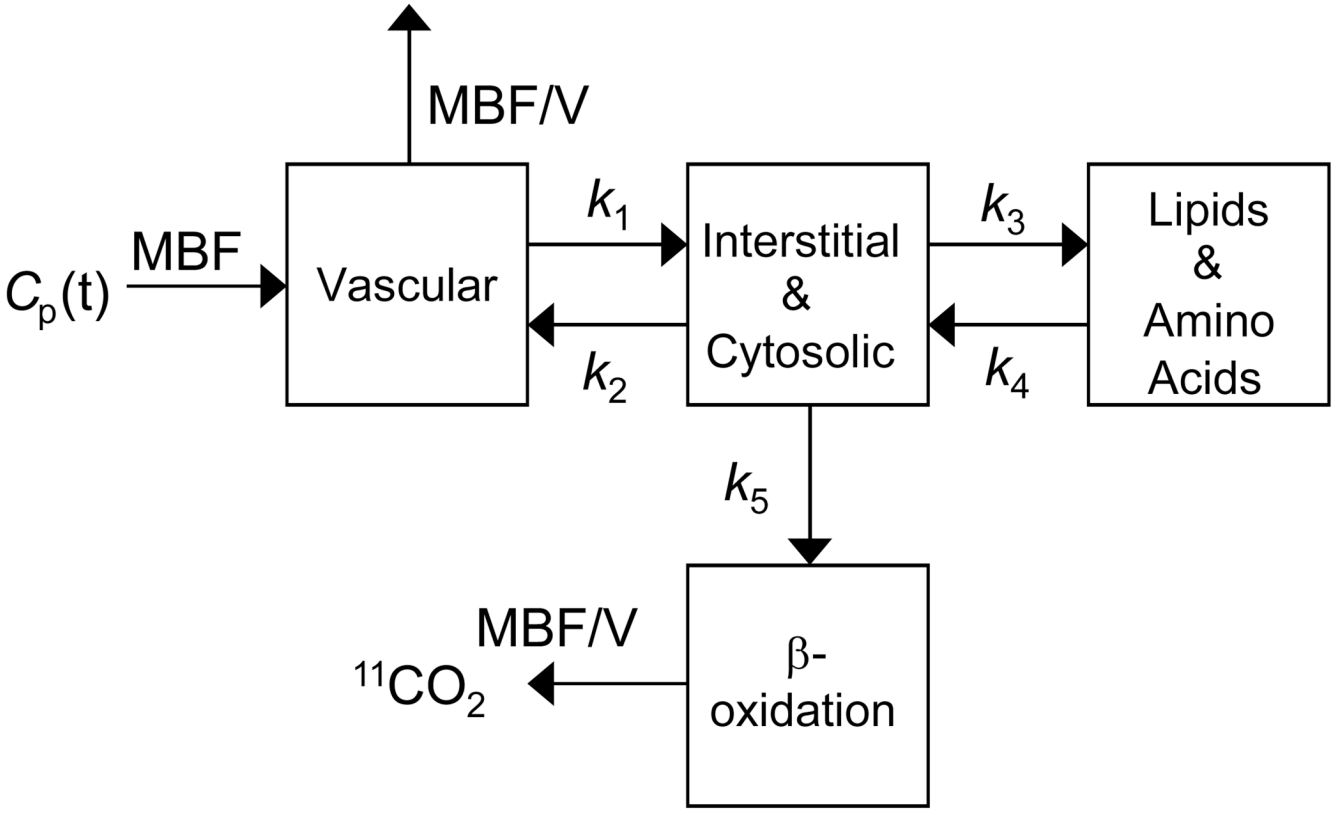

Figure 1.
Compartmental model depicting the kinetics of [^{11}C]Palmitate in tissue. The rate-constants K_1 (/mL/g/min) and k_2 (/min) denote reversible exchange between the vascular compartment while k_3 (/min) and k_4 (/min) denote the exchange between the interstitial & cytosolic compartments and lipids and amino acids compartment. The plasma input function ($C_P(t)$) serves as a forcing function to the model with rate-constant provided by the myocardial blood flow (MBF) and clearance rate-constant MBF/V (V=0.1) [28].

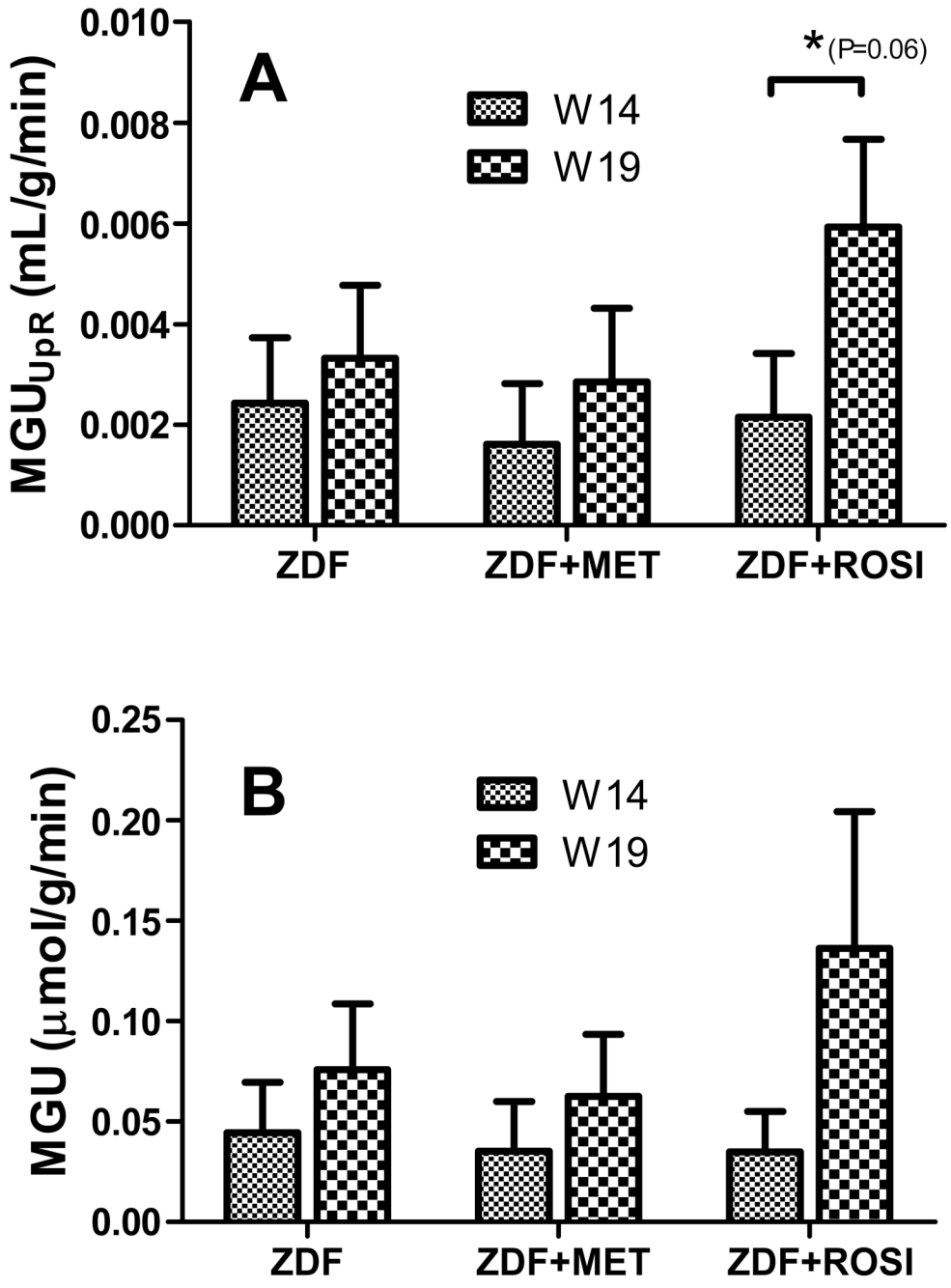

Figure 2.

(A) myocardial glucose utilization uptake rate (MGU_{UpR}) and (B) myocardial glucose utilization (MGU) in untreated (ZDF), Metformin-treated (ZDF+MET) and Rosiglitazone-treated (ZDF+ROSI) at week 14 (W14) and week 19 (W14). MGU_{UpR} represents the intrinsic capacity of the heart to uptake glucose independent of the plasma concentration of glucose ($[Glu]_P$) while MGU is derived by the relation $MGU=MGU_{UpR}*[Glu]_P$. *, denotes that the treatment effect is marginally insignificant compared to untreated rats (P=0.06). All resulted are presented as mean ± 1 SD.

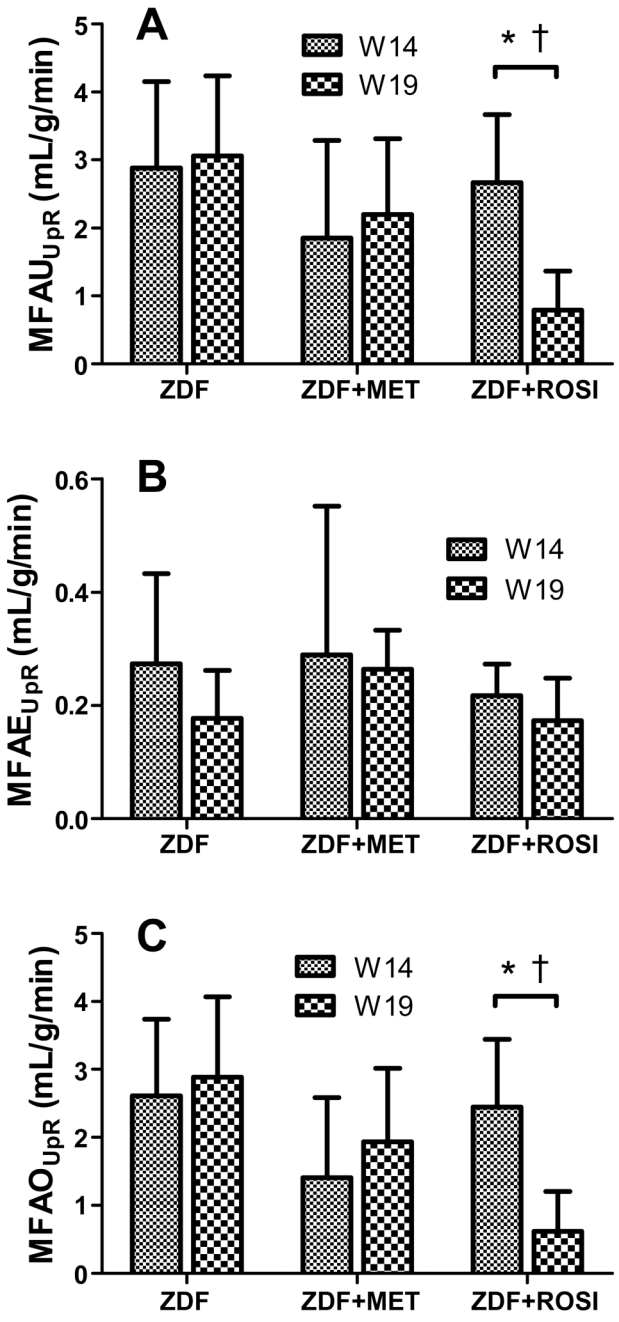

Figure 3.

Myocardial fatty acid utilization measures. Myocardial fatty acid utilization uptake rate ($MFAU_{UpR}$) (A), myocardial fatty acid esterification uptake rate ($MFAE_{UpR}$) (B), and (C) myocardial fatty acid oxidation uptake rate ($MFAO_{UpR}$) in untreated (ZDF), Metformin-treated (ZDF+MET) and Rosiglitazone-treated (ZDF+ROSI) ZDF rats at week 14 (W14) and week 19 (W14). $MFAE_{UpR}$, $MFAO_{UpR}$ and $MFAU_{UpR}$ represents the intrinsic capacity of the heart to oxidize and utilize fatty acids, respectively, independent of the concentration of free fatty acids in plasma ($[FFA]_P$) while MFAO is derived by the relations $MFAO=MFAO_{UpR}*[FFA]_P$. *, denotes that the treatment is significantly better than no treatment; †, denotes that

the Rosiglitazone treatment is significantly better than Metformin treatment. A $P<0.05$ was considered significant. All resulted are presented as mean ± 1 SD.

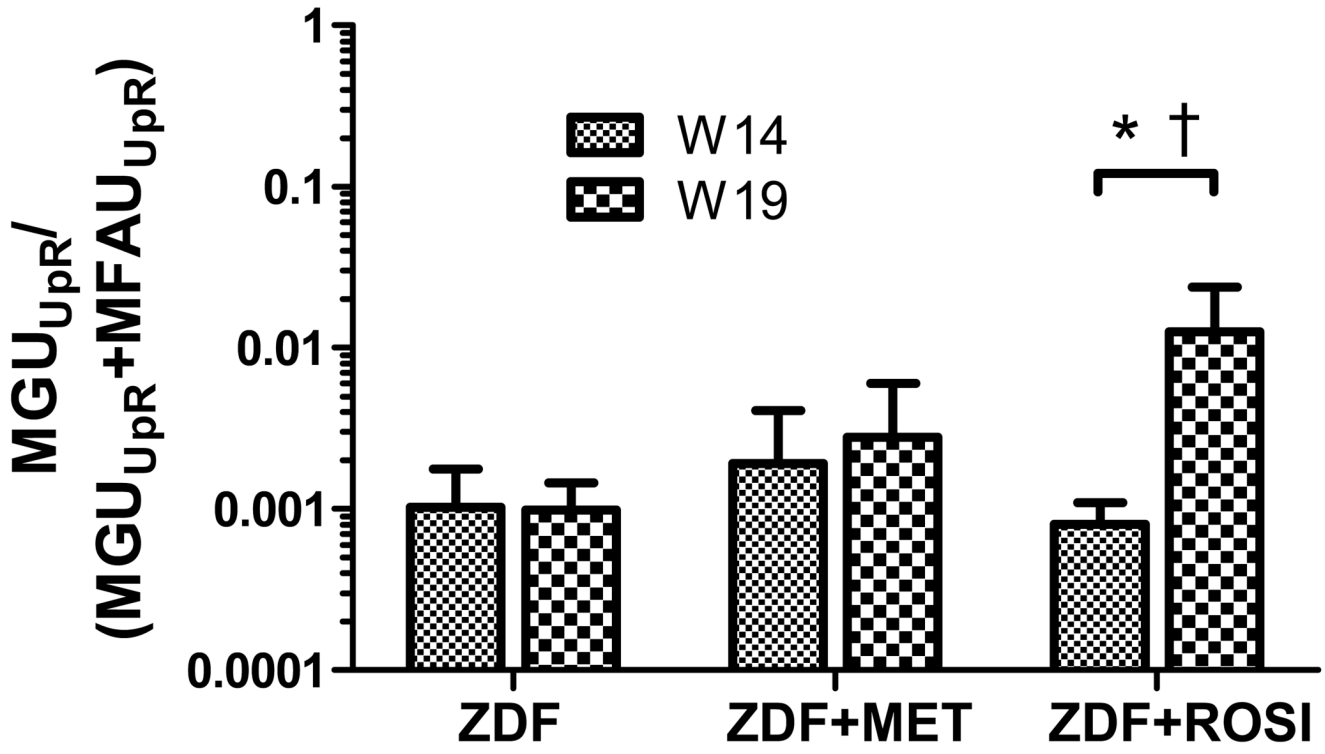

Figure 4.
The fractional net gain in glucose utilization uptake rate in untreated (ZDF), Metformin-treated (ZDF+MET) and Rosiglitazone-treated (ZDF+ROSI) ZDF rats at week 14 (W14) and week 19 (W14). Note: Y-axis is in logarithmic scale. *, denotes that the treatment is significantly better than no treatment; †, denotes that the Rosiglitazone treatment is significantly better than Metformin treatment. A $P<0.05$ was considered significant. All resulted are presented as mean ± 1 SD.

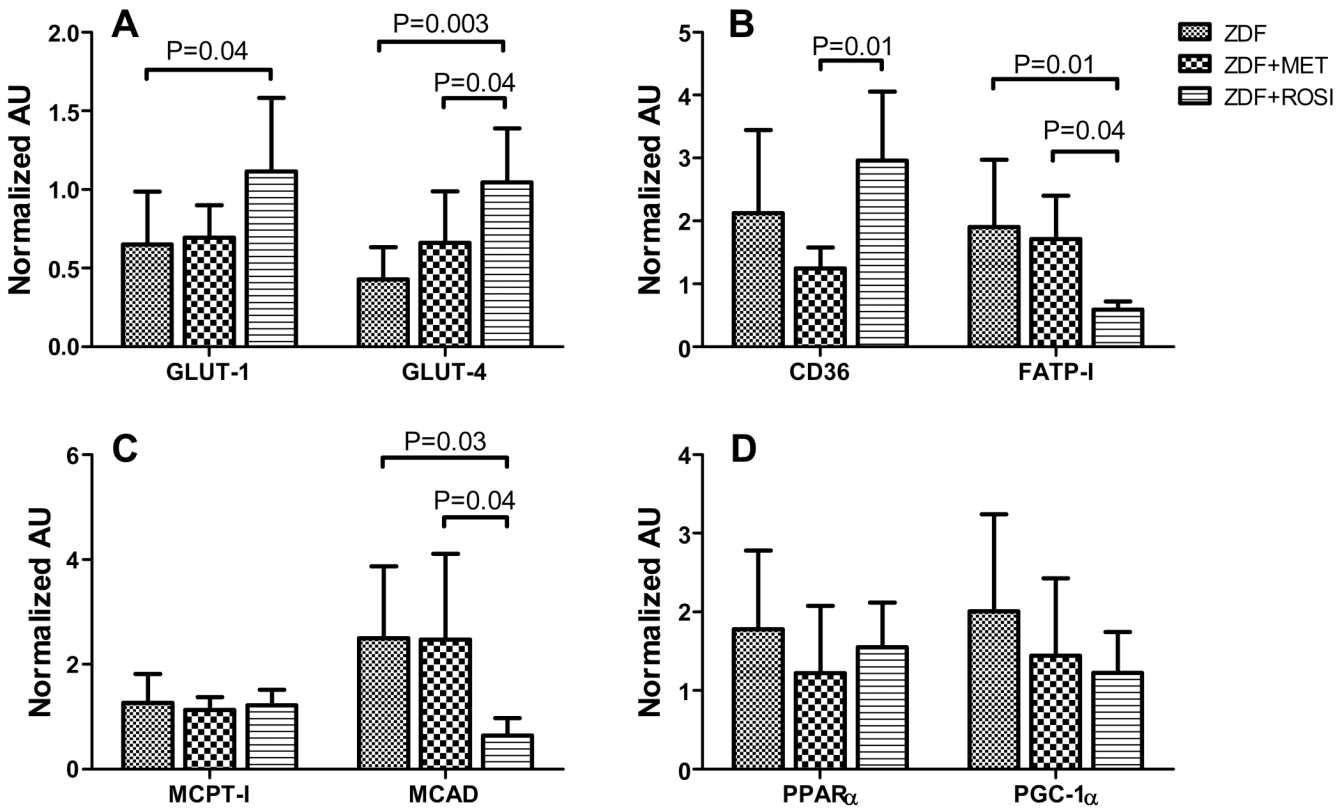

Figure 5.

Gene expression of (A) glucose transporters GLUT1 and GLUT4; (B) Fatty acid transporters FATP-I and CD36; (C) and genes encoding for proteins involved in fatty acid oxidation, namely MCPT-I and MCAD. Legend provided in panel C is applicable to both panels A and B. Significant differences between groups are denoted above bar-plots. A $P<0.05$ was considered significant. AU=Arbitrary Units. All resulted are presented as mean ± 1 SD.

Table 1

Descriptive data, hemodynamics, and plasma substrate levels of untreated and treated ZDF (fa/fa) rats

	ZDF		ZDF+Metformin		ZDF+Rosiglitazone	
	W14	**Δ**	**W14**	**Δ**	**W14**	**Δ**
Weight (g)	316.35±17.66	27.73±11.63*	330.32±50.35	32.08±46.53	328.17±17.56	184.50±32.14†,‡
HR (bpm)	207.17±13.29	−0.75±4.99	216.67±26.34	−22.50±17.80	223.33±34.21	−1.33±13.25
HbA1C (%)	7.72±0.66	−0.33±0.45	6.98±1.36	−1.52±0.55†	7.67±0.50	−3.27±0.39†,‡
Insulin (mU/mL)	26.24±6.97	−8.17±12.58	28.24±15.01	6.31±32.37	42.18±22.13	−14.05±32.92
Glucose (mM)	18.28±4.97	4.30±4.85	22.94±3.38	−1.52±5.33	16.91±5.23	4.89±6.69
FFA (mM)	1.73±0.68	0.19±1.32	2.95±1.12	0.26±1.24	2.91±1.24	−0.88±1.19
MBF (mL/g/min)	5.30±0.92	0.12±1.37	5.12±1.66	0.33±2.84	5.42±2.60	−0.45±2.51
MVO_2 (mmol/g/min)	33.89±6.12	1.46±11.03	30.60±6.14	3.44±8.25	34.31±3.75	8.24±12.15

Average baseline (W14) and change from baseline (Δ).

Values are represented as mean ± 1 standard deviation

*Significantly higher than week 14

†Treatment response significantly higher than no treatment

‡Treatment response significantly higher than Metformin treatment

P-value $P<0.05$ was considered significant

HR, heart rate; HbA1C, glycosylated hemoglobin; FFA, free fatty acids; MBF, myocardial blood flow; MVO_2, Myocardial oxygen consumption

Table 2

Echocardiographic (ECHO) measurements for untreated and treated ZDF (fa/fa) rats

	ZDF		ZDF+Metformin		ZDF+Rosiglitazone	
	W13 (n=6)	**Δ (*v*=4)**	**W13 (n=6)**	**Δ (*v*=6)**	**W13 (n=6)**	**Δ (n=6)**
LVIDd (mm)	9.16±0.32	0.15±0.29	9.13±0.16	0.32±0.42	8.98±0.13	0.93±0.47*,†
LVIDs (mm)	5.53±0.29	0.01±0.14	5.78±0.39	0.19±0.50	5.25±0.48	0.44±0.96
LVM (g)	1.00±0.07	0.05±0.16	1.17±0.10	0.38±0.15*	1.05±0.07	0.42±0.08*
LVMI	3.15±0.17	−0.11±0.47	3.61±0.57	0.70±0.76*,‡	3.21±0.28	−0.32±0.28
FS (%)	39.72±1.72	0.89±1.30	36.70±4.41	0.11±5.24	41.60±5.44	1.19±7.59

Average baseline (W13) and change from baseline (Δ).

Values and Values are represented as mean ± 1 standard deviation

*Treatment response significantly higher than no treatment

†Treatment response significantly higher than Metformin treatment

‡Treatment response significantly higher than Rosiglitazone treatment

P-value $P<0.05$ was considered significant

LVIDd, LV diastolic internal diameter; LVIDs, LV systolic internal diameter; LVM, LV mass; LVMI, LV mass index; FS, fractional shortening

Table 3

Pearson correlation between PET measures of MGU_{UpR}, $MFAO_{UpR}$, and gene expression at W19

		ZDF/ZDF+Met			ZDF/ZDF+Rosi			ZDF/ZDF+MET/ZDF+Rosi		
		ρ	P	N	ρ	P	N	ρ	P	N
MGU_{UpR} vs.	GLUT1	−0.66	0.02698*	9	0.46	0.07531	11	0.40	0.07136	15
	GLUT4	0.01	0.48850	9	0.71	0.00710*	11	0.55	0.01732*	15
$MFAO_{UpR}$ vs.	CD36	0.61	0.01728*	12	−0.08	0.40411	12	−0.09	0.35652	18
	FATP1	0.09	0.39339	11	0.74	0.00441*	11	0.48	0.03046*	16
	mCPT1	0.68	0.00730*	12	0.41	0.09085	12	0.36	0.07338	18
	MCAD	−0.05	0.43995	11	0.71	0.00741*	11	0.38	0.07478	16

*Significant at P<0.05

ρ denotes the Pearson correlation; P, significance value of correlation; N, number of data points; MGU_{UpR}, myocardial glucose utilization uptake rate constant; $MFAO_{UpR}$, myocardial fatty oxidation uptake rate constant